

Optical knife-edge technique for nanomechanical displacement detection

D. Karabacak and T. Kouh^{a)}

Department of Aerospace and Mechanical Engineering, Boston University, Boston, Massachusetts 02215

C. C. Huang

Department of Electrical and Computer Engineering, Boston University, Boston, Massachusetts 02215

K. L. Ekinci^{b)}

Department of Aerospace and Mechanical Engineering, Boston University, Boston, Massachusetts 02215

(Received 5 January 2006; accepted 29 March 2006; published online 11 May 2006)

We describe an optical knife-edge technique for nanomechanical displacement detection. Here, one carefully focuses a laser spot on a moving edge and monitors the reflected power as the edge is displaced sideways. To demonstrate nanomechanical displacement detection using the knife-edge technique, we have measured *in-plane* resonances of nanometer scale doubly clamped beams. The obtained displacement sensitivity is in the $\sim 1 \text{ pm}/\sqrt{\text{Hz}}$ range—in close agreement with a simple analytical model. © 2006 American Institute of Physics. [DOI: 10.1063/1.2203513]

Electromechanical devices are rapidly being miniaturized, following the trend in transistor electronics. Nanometer scale electromechanical devices—usually called nanoelectromechanical systems¹ (NEMS)—have recently been at the focus of applied^{2–4} and fundamental^{5,6} research. In most NEMS-based sensing^{2–4} and metrology,⁶ one drives the nanomechanical element resonantly and detects its subsequent displacement—as the device interacts with its environment. Detection of nanomechanical displacements with high sensitivity, therefore, is vital for reliable NEMS operation.

High frequency NEMS resonators are most commonly realized in the form of doubly clamped beams. At room temperature, displacement detection in nanomechanical doubly clamped beam resonators has been realized efficiently using optical interferometry.^{7,8} In interferometry, one exploits the optical path length change as the center of the nanomechanical beam moves in the *out-of-plane* direction, i.e., *parallel* to the optical axis. However, interferometry becomes ineffective in the widely used beam-gate geometry, where the beam is actuated sideways, i.e., *vertical* to the optical axis.^{9,10} In this letter, we describe an optical technique complementary to interferometry for detecting the *in-plane* nanomechanical motion of a doubly clamped beam. The technique relies upon the change in reflected optical power from the beam as the beam moves inside a Gaussian optical spot; it is essentially a knife-edge technique. Knife-edges are widely used for characterizing optical spots¹¹ and have been implemented in optical beam-deflection based displacement detection.¹²

The nanomechanical resonators used in this work were doubly clamped beams fabricated on a silicon nitride membrane.¹⁰ An electrically isolated side gate was fabricated next to the doubly clamped beam for in-plane electrostatic actuation. To enhance the optical reflectivity, a thin layer of Cr, Al, or Au was thermally deposited on the structures. The film material and the thickness had a large effect on the measured resonance properties. A typical device is shown in Fig. 1(a).

The experiments were performed inside an ultrahigh vacuum (UHV) chamber.⁸ A He–Ne laser ($\lambda=632 \text{ nm}$) was focused on the nanomechanical beam by an objective lens with a numerical aperture of 0.5 resulting in a diffraction limited optical spot of diameter $d=1.2 \text{ }\mu\text{m}$ (measured at full width at half maximum). Figure 1(b) is an illustration showing the beam and the optical spot. The optical spot is offset by a distance x_s from the equilibrium beam center position at $x=0$; the beam center displaces to x_b when excited. In the experiments, the in-plane resonance of the beam was electrostatically actuated and the reflected optical signal was monitored. Using this technique, we measured the in-plane fundamental flexural resonances of six beams with resonance frequencies in the $7 \text{ MHz} < \omega_0/2\pi < 20 \text{ MHz}$ range. Figure 1(c) shows a typical resonance signal at fixed ac and varied dc actuation voltages. The inset displays the dc drive voltage dependence of $\omega_0/2\pi$. This particular device had (beam) dimensions $t \times w \times l = 125 \text{ nm} \times 200 \text{ nm} \times 14 \text{ }\mu\text{m}$ and beam-gate separation $g=130 \text{ nm}$. The quality factor of the resonator was $Q \approx 800$.

In the knife-edge technique, the quantity that determines the displacement signal is the change in reflected optical power P_r with respect to the center position x_b of the nanobeam [see Fig. 1(b)], $\mathcal{R}=(1/P_0)/(\partial P_r/\partial x_b)$. We shall call \mathcal{R} the responsivity, which is normalized with respect to the incident power P_0 . The resonance measurements such as those shown in Fig. 1(c) were performed at a point of maximum available responsivity \mathcal{R}_0 . This optimal operation point x_{s0} was found by changing the optical spot position x_s with respect to the nanobeam and finding the point of maximum signal. While this approach resulted in the best signal-to-noise ratio, it did not allow the conversion of the photocurrent into an absolute displacement.

In order to determine the (normalized) absolute \mathcal{R}_0 (in units of μm^{-1}), we use the following first-pass approximation: a displacement x_b of the beam center relative to the optical spot ought to give rise to the same measured power change as a displacement x_s of the spot relative to the stationary beam, if $x_b=-x_s$. The approximation that follows is

^{a)}Present address: Department of Physics, Kookmin University, Seoul 136-702, Korea.

^{b)}Author to whom correspondence should be addressed; electronic mail: ekinci@bu.edu

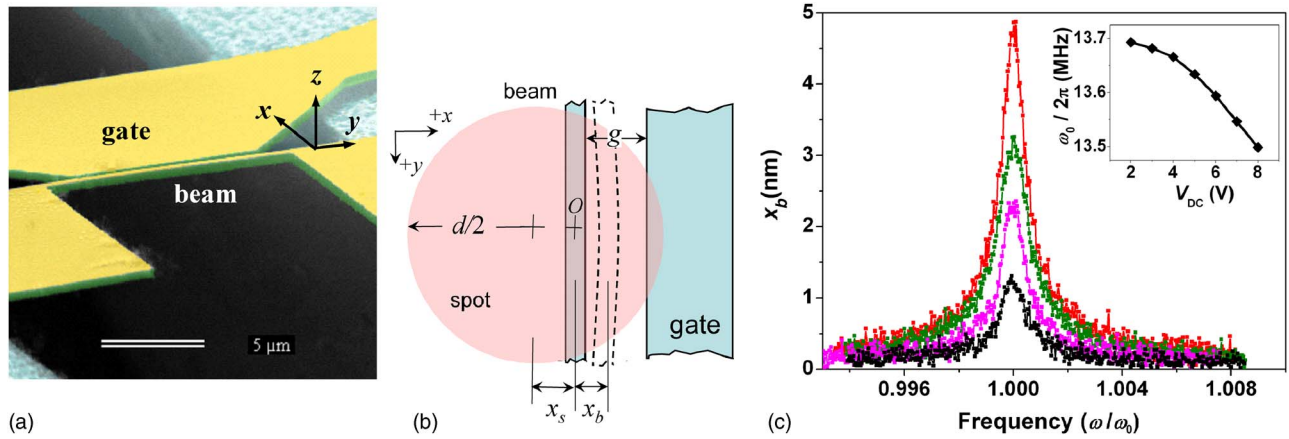


FIG. 1. (Color online) (a) Scanning electron micrograph of a typical doubly clamped silicon nitride beam with a side gate. (b) An illustration of the experiment. The optical spot is focused at an offset of x_s from the beam center of the NEMS resonator. The NEMS center displacement from equilibrium is x_b ; in the illustration, the displacement of the beam is exaggerated. The equilibrium gap is g . The origin is at the center of the beam. (c) In-plane fundamental flexural resonance of a $t \times w \times l = 125 \text{ nm} \times 200 \text{ nm} \times 14 \text{ } \mu\text{m}$ and $g = 130 \text{ nm}$ beam for varying dc drive amplitude V_{dc} . The inset displays the change in the resonance frequency with V_{dc} .

$$\mathcal{R}_0 \approx - \left. \frac{1}{P_0} \frac{\partial P_r}{\partial x_s} \right|_{x_s=x_{s0}}. \quad (1)$$

$$P_r(x_s) \approx \int_{-\infty}^{+\infty} \int_{-\infty}^{+\infty} I(x,y) R(x,y) dx dy. \quad (2)$$

We note that this is valid only if (i) the power reflected from the side gate is negligible and (ii) the beam is long so that the curvature around the beam center during motion is small. Thus, an approximate \mathcal{R}_0 value can be determined by measuring P_r as a function of x_s and finding $\partial P_r / \partial x_s$.

Experimentally, we carefully scanned the optical spot over our devices using a precision translation stage and recorded $P_r(x_s)$. We performed these spot-scan measurements on two representative devices with different dimensions in order to understand the limits of the above-described approximation. The devices, henceforth D1 and D2, had identical thicknesses and lengths: $t = 125 \text{ nm}$ and $l = 14 \text{ } \mu\text{m}$. D1 had $w = 500 \text{ nm}$ and $g = 500 \text{ nm}$; D2 had $w = 200 \text{ nm}$ and $g = 130 \text{ nm}$. Note that $g \sim d/2$ for D1, but $g < d/2$ for D2. The inset of Fig. 2(a) displays $P_r(x_s)$ for D1. Note that (i) at large negative values of x_s , no light is reflected; (ii) as the spot is scanned over the beam, the reflected power increases; and (iii) when the spot is over the gate (large positive x_s), all the incoming light essentially reflects back. The main figure [Fig. 2(a)] is the normalized numerical derivative of $P_r(x_s)$ with respect to x_s for D1. Similar plots for D2 are presented in the inset and the main body of Fig. 2(b). Note the presence of two maxima in Fig. 2(a) as opposed to the single peak in Fig. 2(b). As discussed in detail below, the two separate peaks indicate that the gate contribution to the reflected power is negligible around x_{s0} . Thus, Eq. (1) is accurate and \mathcal{R}_0 is readily accessible in devices such as D1 where $g \sim d/2$. The extraction of \mathcal{R}_0 from a single peak (D2) requires further attention (see discussion below).

Let us now take a brief analytical look at $P_r(x_s)$ and $\partial P_r / \partial x_s$. $P_r(x_s)$ can be determined by an integral of the Gaussian intensity profile $I(x,y) \approx I_0 e^{-2(x-x_s)^2/d^2} e^{-2y^2/d^2}$ over the reflecting portions of the device surface [see Fig. 1(b)], if diffraction effects are neglected.¹¹ The reflected power thus becomes

The function $R(x,y)$, in the simplest approximation, is unity if the point is on the device or the gate and zero everywhere else. The results obtained from Eq. (2) are presented as the dashed lines in both Figs. 2(a) and 2(b). The spot size d used in the calculations was determined from separate knife-edge measurements. The data and the calculation are in good qualitative agreement. We estimate that the discrepancy in the magnitude of the peaks can be attributed to diffraction effects at this scale. In a more rigorous finite element calculation (not shown), the agreement of the signal magnitude was to within 10% of the experimental data.

We now return to the problem of determining \mathcal{R}_0 from spot-scan measurements, i.e., from $\partial P_r / \partial x_s$ curves of Figs. 2(a) and 2(b). In devices where $g \geq d/2$, the light reflecting from the gate is not significant around $x_s \approx x_{s0}$. Thus, Eq. (1) remains valid. Note also that for $g \geq d/2$, the spot scan will reveal two peaks optically resolving both the beam and the gate. In contrast, in devices where the gate lies within the spot (D2), spot-scan experiments *overestimate* \mathcal{R}_0 . During spot scans around $x_s \approx x_{s0}$, $P_r(x_s)$ variation is not only due to the *relative* position shift of the nanobeam and the spot but also due to the change in the amount of light reflecting from the side gate. The gate contribution, however, is irrelevant to the displacement signal of the resonator. Thus, with decreasing g , the approximation in Eq. (1) becomes less accurate. One additional complication is that the two separated peaks merge into a single peak when the gate is nearby [Fig. 2(b)]. This indicates that the point of maximum signal may *not* correspond to the maximum $\partial P_r / \partial x_s$. In Fig. 2(b), we present a second calculation for D2 without the gate (solid line), which indicates that the inaccuracy in \mathcal{R}_0 due to the gate can be as much as 30%. In short, the knife-edge technique is rather accurate in *absolute* displacement detection in devices where the gate is far away in comparison to the spot size. Otherwise a combination of numerical and experimental analyses, as presented here, can be used to obtain an estimate for the absolute displacement.

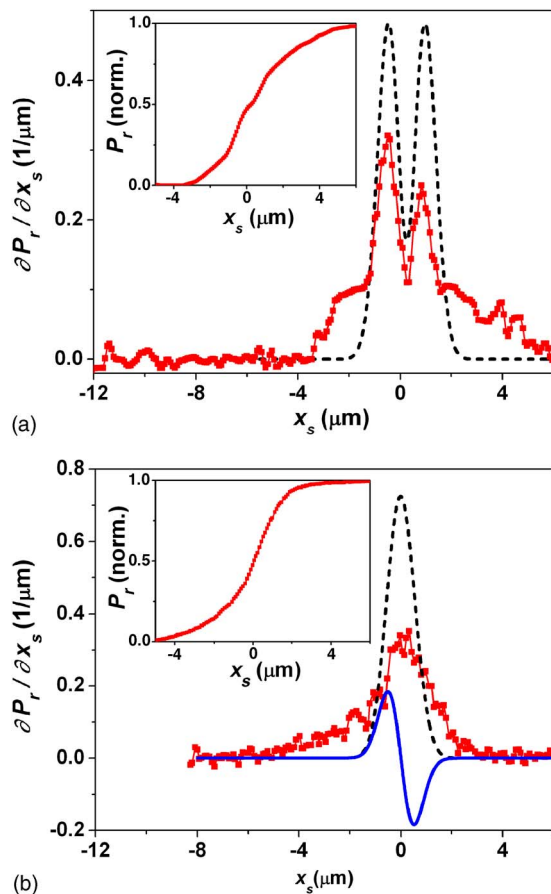


FIG. 2. (Color online) Normalized optical responsivity of NEMS devices, with dimensions of (a) $w=500$ nm and $g=500$ nm and (b) $w=200$ nm and $g=130$ nm. The inset shows the normalized reflected power P_r as a function of the spot position x_s . Analytical calculation results for $\partial P_r / \partial x_s$ are plotted as dashed lines. In (b), the solid line shows $\partial P_r / \partial x_s$ without the contribution of the gate.

The \mathcal{R}_0 values in our measurements were in the range $\mathcal{R}_0 \sim 0.2 \mu\text{m}^{-1}$ in subwavelength devices. This corresponded to a displacement sensitivity of $\sim 1 \text{ pm}/\sqrt{\text{Hz}}$ at a power $P_0 \approx 300 \mu\text{W}$. In our experiments, the sensitivity was limited by the amplifier noise. These values are comparable or better than those obtained in our previously reported optical interferometry measurements for out-of-plane motion.⁸ For a device that had $w=200$ nm, under identical incident power and spot size values, Michelson interferometry and Fabry-Perot interferometry resulted in $\mathcal{R}_0 \sim 0.01 \mu\text{m}^{-1}$ corresponding to a noise floor of $\sim 20 \text{ pm}/\sqrt{\text{Hz}}$.⁸

To further assess the limits of the knife-edge detection technique, we calculated \mathcal{R}_0 as a function of effective device size w and optical spot size d . In these calculations, we assumed that the gate was far away. The results of this calculation are presented in Fig. 3. Here, we plotted equal responsivity contours as a function of w and d . The results clearly demonstrate that detection sensitivity will deteriorate as the device size is reduced or as the optical spot is enlarged.

NEMS resonators on membranes with in-plane motion can be of further value at large optical detection power. By using light at $\lambda=1550$ nm, for instance, the incident power

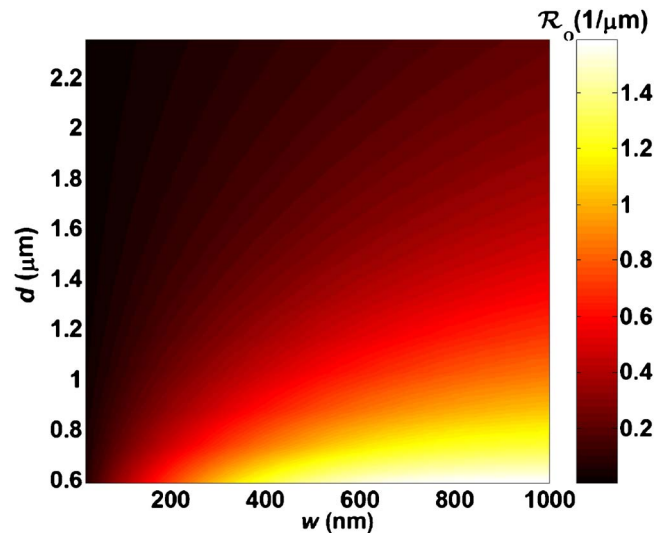


FIG. 3. (Color online) Peak responsivity \mathcal{R}_0 contour plot as a function of both beam width w and spot diameter d .

might be increased by an order of magnitude—possibly enabling shot noise limited optical detection. Once in the shot noise limit, removing the substrate can further improve the signal-to-noise ratio by reducing the background in the optical signal.^{7–9}

In summary, we have described an optical knife-edge technique for sensitive displacement detection in nanomechanical beams. The technique is complementary to optical interferometry in that it allows in-plane displacement detection. The experimental results are in good agreement with a simple analytical model.

The authors gratefully acknowledge support from the NSF under Grant Nos. ECS-210752, BES-216274, and CMS-324416. The authors thank O. Balogun for a critical reading of the manuscript.

¹M. L. Roukes, Phys. World **14**, 25 (2001); H. G. Craighead, Science **290**, 1532 (2000).

²K. L. Ekinci, X. M. H. Huang, and M. L. Roukes, Appl. Phys. Lett. **84**, 4469 (2004); K. L. Ekinci and M. L. Roukes, Rev. Sci. Instrum. **76**, 061101 (2005).

³B. Ilic, H. G. Craighead, S. Krylov, W. Senaratne, C. Ober, and P. Neuzil, J. Appl. Phys. **95**, 3694 (2004).

⁴X. M. H. Huang, M. Manolidis, S. C. Jun, and J. Hone, Appl. Phys. Lett. **86**, 143104 (2005).

⁵M. P. Blencowe, Contemp. Phys. **46**, 249 (2005).

⁶M. D. LaHaye, O. Buu, B. Camarota, and K. C. Schwab, Science **304**, 74 (2004); R. G. Knobel and A. N. Cleland, Nature (London) **424**, 291 (2003).

⁷D. W. Carr, L. Sekaric, and H. G. Craighead, J. Vac. Sci. Technol. B **16**, 3821 (1998).

⁸T. Kouh, D. Karabacak, D. H. Kim, and K. L. Ekinci, Appl. Phys. Lett. **86**, 013106 (2005); D. Karabacak, T. Kouh, and K. L. Ekinci, J. Appl. Phys. **98**, 124309 (2005).

⁹C. Meyer, H. Lorenz and K. Karrai, Appl. Phys. Lett. **83**, 2420 (2005).

¹⁰T. Kouh, O. Basarir, and K. L. Ekinci, Appl. Phys. Lett. **87**, 113112 (2005).

¹¹A. H. Firester, M. E. Heller, and P. Sheng, Appl. Opt. **16**, 1971 (1976); J. M. Khosrofi and B. A. Garetz, Appl. Opt. **22**, 3406 (1983).

¹²J. W. Wagner, Phys. Acoust. **19**, 201 (1990).